Type Ia Supernovae: Progenitors and Peculiarity

K. Nomoto*, M. Tanaka*, K. S. Kawabata†, D. K. Sahu** and G. C. Anupama**

*Department of Astronomy, University of Tokyo, Bunkyo-ku, Tokyo 113-0033, Japan
†Hiroshima Astrophysical Science Center, Hiroshima University, 1-3-1 Kagamiyama, Higashi-Hiroshima, Hiroshima 739-8526, Japan
**Indian Institute of Astrophysics, II Block Koramangala, Bangalore 560034, India

Abstract.
Among the controversial issues on Type Ia supernovae (SNe Ia), we discuss (1) the evolutionary paths of the progenitor systems to SNe Ia, especially, the thermal stability of hydrogen shell burning in accreting white dwarfs, and (2) SN 2005hk which belongs to the very peculiar 2002cx-like group of SNe Ia. For SN 2005hk, we show our observations of the light curve and late time spectra, and present a preliminary model for the light curve to confirm it is quite a low energy explosion.

Keywords: supernova, white dwarf
PACS: 97.60.Bw, 26.30.+k, 97.20.Rp

INTRODUCTION

Type Ia supernovae (SNe Ia) are characterized by the lack of hydrogen and the prominent Si line in their spectra near maximum light and widely believed to be thermonuclear explosions of mass-accreting white dwarfs in binary systems [8]. SNe Ia have been used as a "standard candle" to determine cosmological parameters thanks to their relatively uniform light curves and spectral evolution. SNe Ia are also the major sources of Fe in the galactic and cosmic chemical evolution.

Despite such importance, there have been several serious controversial issues [e.g., 18, 13]. Among them, we pick up two issues.

(1) Stability of hydrogen shell burning on the surface of the accreting white dwarfs.

(2) The nature of very peculiar group of SN 2002cx-like SNe Ia, based on our own observations.

EVOLUTIONARY PATHS TO TYPE IA SUPERNOVAE

In the most popular model, the Chandrasekhar mass model, a C-O white dwarf accretes mass until it grows in mass to $M = 1.38\ M_\odot$, then explodes as an SN Ia [e.g., 15, 17]. To find a path to SNe Ia is to find a way for a C-O white dwarf to increase its central density and temperature to C ignition as the Chandrasekhar limit is approached. If the mass donor is a normal star, the stability of the hydrogen burning shell in the accreting white dwarf is crucial for its evolution.

A hydrogen-shell burning is ignited in an accreting white dwarf when a certain amount of hydrogen-rich matter is accumulated in the envelope. The shell burning is unstable to

CP924, *The Multicolored Landscape of Compact Objects and their Explosive Origins - Cefalù 2006,*
edited by T. Di Salvo, L. A. Antonelli, G. L. Israel, L. Piersanti, A. Tornambè, L. Burderi, F. Fiore, G. Matt, and M. T. Menna

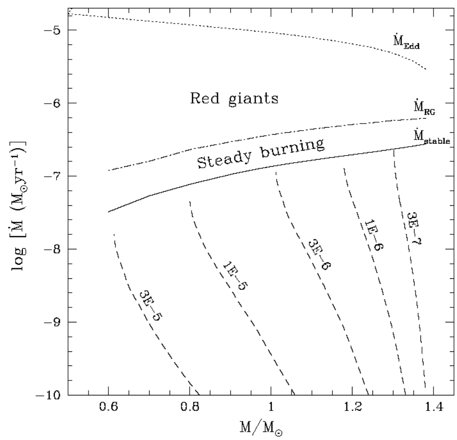

FIGURE 1. The properties of the steady H-burning shells in accreting white dwarfs are shown in the white dwarf mass M – accretion-rate $\dot{M}$ plane [19]. If the accretion rate is lower than the solid line of $\dot{M}_{\rm stable}$, H-burning shells are thermally unstable. A dashed line traces the locus of the envelope mass $\Delta M_{\rm env}/M_\odot$ of the steady burning models. In the area between the solid ($\dot{M}_{\rm stable}$) and dash-dotted ($\dot{M}_{\rm RG}$) lines, the H-burning shell burns steadily and stably. Above the dash-dotted line for $\dot{M}_{\rm RG}$, the stellar envelope is expanded to a red-giant size and a strong wind occurs. Dotted line indicate the Eddington accretion rate $\dot{M}_{\rm Edd}$ as a function of M.

flash if the accretion rate is lower than a critical rate. The flash is stronger if the white dwarf is cooler and the accretion is slower [20, 25, 3]. If the shell flash is strong enough to trigger a nova outburst, most part of the envelope is lost from the system. Moreover, a part of the original white dwarf matter is dredged up and lost in the outburst wind. Therefore, the white dwarf mass decreases after one cycle of nova outburst [e.g., 22].

If the accretion rate $\dot{M}$ is high enough, on the other hand, the shell burning is stable and the mass of the white dwarf increases with accretion. Thus, the critical accretion rate $\dot{M}_{\rm stable}$, above which hydrogen shell burning is stable, is an important physical value for the evolution of accreting white dwarfs.

Thermal Stability of Hydrogen-Shell Burning

The stability of a nuclear shell burning in an accreting white dwarf has been extensively studied in connection with nova outbursts. Sienkiewicz [24] obtained the stability boundary by examining thermal stability of steady-state models for accreting white dwarfs of various masses. The stability boundary, which is $\dot{M}_{\rm stable} \simeq 10^{-7} M_\odot {\rm yr}^{-1}$ at $M = 0.8 M_\odot$ and higher for more massive white dwarfs, is consistent with fully time dependent calculations [e.g., 20, 25].

Recently, Starrfield et al. [26] (hereafter S04) published new models of accreting white dwarfs called “surface hydrogen burning” models. They argued that if a very hot white dwarf after a nova outburst started accreting hydrogen-rich matter, it developed surface hydrogen burning that stably converts hydrogen into helium and helium into heavier elements; then, the white dwarf mass could grow to the Chandrasekhar limit. They obtained such "surface hydrogen burning" models for accretion rates ranging from 1.6×10^{-9} to $8.0 \times 10^{-7} M_\odot$ yr^{-1}, and identified these models as supersoft X-ray sources. The properties of their models, however, clearly contradict previous results of evolutionary and steady-state models [e.g., 24].

Nomoto et al. [19] (hereafter NSKH) have shown that the contradictory properties of the "surface hydrogen burning" models result from too coarse zoning for the envelope structure. NSKH have first re-calculated steady-state models for various accretion rates and white dwarf masses, and examined the thermal stability of these models to confirm the results of Sienkiewicz [24]. Then NSKH examined the "surface hydrogen burning" models by S04 and discussed the reason for the discrepancy between S04 models and the previous results.

The stability is determined by the hydrostatic readjustment $\delta \ln P/\delta s (< 0)$ due to expansion (for $\delta s > 0$), which depends on on the following two factors.

(1) *Geometry*: In the extremely thin shell, the pressure at the bottom of the thin envelope is determined as:

$$P = \frac{GM^2(1-q)}{4\pi R^4}, \tag{1}$$

where R is the radius of the white dwarf, and P is determined only by the column density above the radius r. Therefore, the effect of expansion for $\delta \ln P/\delta s$ is too small to cool the shell and to stabilize nuclear burning. This is the main reason for thin shell burning to be unstable, being the case for low $\dot{M}$. For high $\dot{M}$, entropy at the burning shell is larger, thus leading to a more extended envelope. Then the effect of hydrostatic readjustment (expansion) is larger and tends to stabilize nuclear shell burning.

(2) *Equation of State*: If electrons are degenerate, P depends only weakly on T, which makes the effect of expansion too small to stabilize nuclear burning upon $\delta T > 0$. This is the case for low $\dot{M}$ and thus low s at the burning shell. On the contrary, for high $\dot{M}$ and L, especially, near their RG values, radiation pressure is important and its large T sensitivity stabilizes shell burning.

At $L_{\rm stable} < L < L_{\rm RG}$ (or $\dot{M}_{\rm stable} < \dot{M} < \dot{M}_{\rm RG}$), therefore, these combined effects of radiation pressure and the extended envelope structure lead to stable burning. This is why $\dot{M}_{\rm stable}$ is smaller than $\dot{M}_{\rm RG}$ by only a factor of ~ 2.3 - 2.7.

Figure 1 summarizes the properties of steady-state models accreting hydrogen-rich matter. The vertical axis is the accretion rate $\dot{M}$ and the horizontal axis is the white dwarf mass M. The model properties are classified as follows:

(1) The models are thermally unstable in the area below the solid line to show $\dot{M}_{\rm stable}$. The dashed line indicates the loci where the envelope mass $\Delta M_{\rm env}$ is constant; the value attached to each dashed line indicates $\Delta M_{\rm env}/M_\odot$.

For given M and $\dot{M}$, the envelope masses of these steady-state models are smaller than the envelope masses of the "ignition" models given in Figure 9 in Nomoto[15] because of the higher entropy in the steady-state models than th 'ignition" models (see [19] for more details).

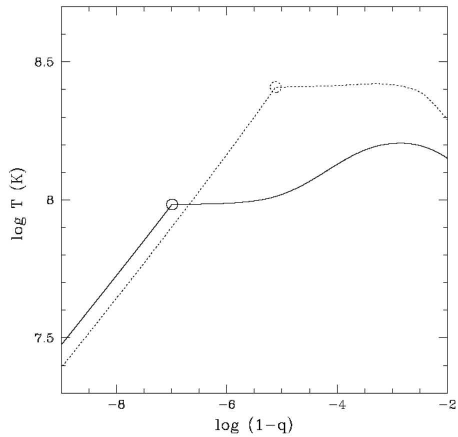

FIGURE 2. Runs of internal temperature against $\log(1-q)$, where $q \equiv M_r/M$. The solid line is for the steady-state model of $M = 1.35 M_\odot$ accreting hydrogen-rich matter at a rate of $1.6 \times 10^{-7} M_\odot$ y^{-1}. The dotted line is for a model of $M = 1.35 M_\odot$ accreting hydrogen-rich matter at the same rate as above but the hydrogen-rich envelope mass is arbitrarily set as $\Delta M_{\rm env} = 10^{-5} M_\odot$. The open circle indicates the bottom of the hydrogen-rich envelope, i.e., the location of hydrogen burning shell.

(2) In the area above the solid line of $\dot{M}_{\rm stable}$, accreting white dwarfs are thermally stable so that hydrogen burns steadily in the burning shell.
(3) Above the dash-dotted line for $\dot{M}_{\rm RG}$, the accreted matter is accumulated faster than consumed into He by H-shell burning. As a result the accreted matter is piled up to form a red-giant size envelope [16].

On "Surface Hydrogen Burning" Models

S04 claimed that their "surface hydrogen burning" models of mass accreting $1.25 M_\odot$ and $1.35 M_\odot$ white dwarfs are thermally stable for accretion rates ranging from $1.6 \times 10^{-9} M_\odot$ yr^{-1} to $8.0 \times 10^{-7} M_\odot$ yr^{-1}. The stability property of NSKH steady-state models, however, differs from that of their models. NSKH models indicate that the hydrogen burning shell in the $1.35 M_\odot$ model is thermally unstable if the accretion rate is less than $2.5 \times 10^{-7} M_\odot$ yr^{-1} ($2.1 \times 10^{-7} M_\odot$ yr^{-1} for $1.25 M_\odot$).

Such a discrepancy is caused by the extremely coarse zoning adopted in S04's computations. S04 adopted a surface zone mass of $10^{-5} M_\odot$, which is much larger than the entire envelope mass of the steady-state models of $M = 1.35 M_\odot$ and $1.25 M_\odot$ as seen in Figure 1. This means that the "surface zone" is much deeper than the realistic hydrogen-rich envelope of the steady-state model corresponding to the same white dwarf mass and the accretion rate.

S04 also wrote that the mass accretion onto the hot white dwarf just after a nova explosion leads to a stable surface hydrogen burning. However, in simulating the mass ejection by the nova explosion, S04 removed the outer meshes without rezoning and exposed the inner coarsely-zoned layers on the surface. This is the reason why the coarse zones are set near the surface in S04.

Figure 2 shows runs of temperature in the interior of two white dwarf models of $M = 1.35M_\odot$ accreting hydrogen-rich matter at a rate of $\dot{M} = 1.6 \times 10^{-7} M_\odot$ yr^{-1}. The abscissa is $\log(1-q)$ with $q \equiv M_r/M$, which is almost equivalent to $\log P$ because the pressure P at M_r in the thin envelope is well-approximated by equation (1). In Figure 2, the sudden change in the temperature gradient at $\log T$(K) = 7.98 (solid line) and 8.41 (dashed line) indicates the bottom of the hydrogen-rich envelope and hence the location of the hydrogen-burning shell. The temperature below the burning shell is almost constant, and decreases toward the deeper layer because of the neutrino cooling in the electron-degenerate core.

(1) The solid line in Figure 2 shows the steady-state model, in which the mass of the hydrogen-rich envelope $\Delta M_{\rm env}$ is determined from the requirement that the hydrogen-burning shell at the bottom of the envelope consume hydrogen at the same rate as of accretion. The resulting envelope mass of this model is $\Delta M_{\rm env} = 1.4 \times 10^{-7} M_\odot$.

(2) The dotted line shows the model having the same white dwarf mass and accretion rate as the above model but the mass of the hydrogen-rich envelope is artificially set to be $\Delta M_{\rm env} = 10^{-5} M_\odot$, which is the same as the "surface zone mass" adopted by S04. The pressure given by equation (1) and thus the temperature are much higher ($\log T$(K) = 8.41) than those of the steady-state model ($\log T$(K) = 7.98). The temperature is comparable to that of the surface zone of S04, from which we see the reason why S04 obtain very high temperature at the "surface zone". They treated the envelope between the region of $\log(1-q) \sim (-5)-(-22)$ by a single mass zone, while our steady-state models resolve the H-rich envelope with ~ 50 mass zones. Obviously, the zoning adopted by S04 is too coarse to obtain a physically realistic stellar model.

In the heavy envelope model, the temperature at the hydrogen burning shell is so high that all accreted hydrogen burns in one typical time step to compute mass accretion, as S04 states "it takes less time than the time step ($\sim 2 \times 10^6$ s) for all the infalling hydrogen to burn to helium in this zone". In this case, the nuclear energy generation rate $\varepsilon_{\rm n}$ is determined not by the temperature-dependent nuclear reaction rate but by the supplying rate of nuclear fuel as

$$\varepsilon_{\rm n} = \frac{XQ\dot{M}}{\Delta M_{\rm env}}. \tag{2}$$

Despite such a high temperature as $\log T$(K) = 8.41, the energy generate rate thus determined is $\varepsilon_{\rm n} = 2.2 \times 10^9$ ergs g^{-1} s^{-1}, which is much lower than the $\beta-$limited reaction rate of the hot CNO cycle $\varepsilon_\beta = 6 \times 10^{13} (X_{\rm CNO}/0.01)$ ergs g^{-1} s^{-1}. Because $XQ\dot{M}/\Delta M_{\rm env}$ is constant, being independent of the temperature, the nuclear burning is stable. In other words, the assumed envelope mass $\Delta M_{\rm env}$ is too large and hence the temperature at the nuclear burning shell is too high for the mass accretion rates they assumed. All the accreted hydrogen-rich matter should have been consumed long before it is pushed into a layer as deep as $M - M_r \sim 10^{-5} M_\odot$ [14].

White Dwarf Winds and Supersoft X-ray Sources

NSKH have reinvestigated the properties of accreting white dwarfs by constructing steady-state models, in which hydrogen shell burning consumes hydrogen at the same rate as the white dwarf accretes it. NSKH have confirmed that these steady models are stable only when the accretion rate is higher than $\dot{M}_{\rm stable}$ in equation (3).

NSKH results contradict the "surface hydrogen burning" models by S04[26] who found quiescent stable hydrogen burning for a wide range of accretion rates down to $\dot{M} \sim 10^{-9} M_\odot$ yr^{-1}. NSKH have shown that quiescence of "surface hydrogen burning" results from the too large zone mass ($\sim 10^{-5} M_\odot$) in the outer part of the numerical models, and that hydrogen burning must occur in a much more superficial layer ($\sim 10^{-7} M_\odot$).

NSKH have shown that the positions on the HR diagram of most of the luminous supersoft X-ray sources are consistent with the white dwarfs accreting matter at rates high enough for hydrogen shell burning to be thermally stable.

NSKH results support the scenario that the progenitor white dwarfs for SNe Ia can grow their masses to the Chandrasekhar mass by accreting hydrogen-rich matter at a rate as high as $\dot{M} \gtrsim 10^{-7} - 10^{-6} M_\odot$ yr^{-1} [e.g., 11, 6, 7, 18].

We should note that if the white dwarfs undergoing accretion only in the range of $\dot{M}_{\rm stable} < \dot{M} < \dot{M}_{\rm RG}$ could become SNe Ia, it might be difficult to explain the SN Ia rate. Accretion at such a high rate as $\dot{M} > \dot{M}_{\rm stable}$ has been shown to increase the white dwarf radius to a red-giant size [16]; this could lead to the formation of a common envelope and prevent further mass accretion onto the white dwarf.

This problem for $\dot{M} > \dot{M}_{\rm stable}$ has been resolved by the strong white dwarf wind models [6, 7]. If the wind is sufficiently strong, the white dwarf radius stays small enough to avoid the formation of a common envelope. Then steady hydrogen burning increases its mass at a rate $\dot{M}_{\rm RG}$ by blowing the extra mass away in a wind.

When the mass transfer rate decreases below this critical value, optically thick winds stop. If the mass transfer rate further decreases below $\dot{M}_{\rm stable}$, hydrogen shell burning becomes unstable to trigger a mild flashes but still burns a large enough fraction of accreted hydrogen to increase M to SNe Ia; this would correspond to recurrent novae [e.g., 5].

Therefore, SNe Ia can occur for a wide range of $\dot{M}$, and "surface hydrogen burning" is not necessary to enlarge the possible $\dot{M}$ range for SNe Ia. Two types of binary systems can provide such high accretion rates, i.e., (1) a white dwarf and a lobe-filling, more massive (typically $\sim 2-4 M_\odot$), slightly evolved main-sequence or sub-giant star, and (2) a white dwarf and a lobe-filling, less massive (typically $\sim 1 M_\odot$), red-giant [6, 7].

This scenario predicts the presence of several types of circumstellar matter around the binary system, which are characterized various wind velocities $v_{\rm w}$: (1) white dwarf winds with such high velocities as $v_{\rm w} \sim 1000$ km s^{-1}, (2) slow dense matter stripped off the companion star by the white dwarf wind, (3) slow wind matter ejected from a red-giant, and (4) moderate wind velocities blown from the main-sequence star. The high velocity white dwarf winds (1) at a rate of $\dot{M} \sim 10^{-6} M_\odot$ yr^{-1} is consistent with the constraints of $\dot{M} <\sim 3 \times 10^{-8} M_\odot$ yr^{-1} set by radio observations where $v_{\rm w} \sim 10$ km s^{-1} is assumed. Circumstellar matter found for SN 2002ic may be explained with the slow dense stripped-off matter (2).

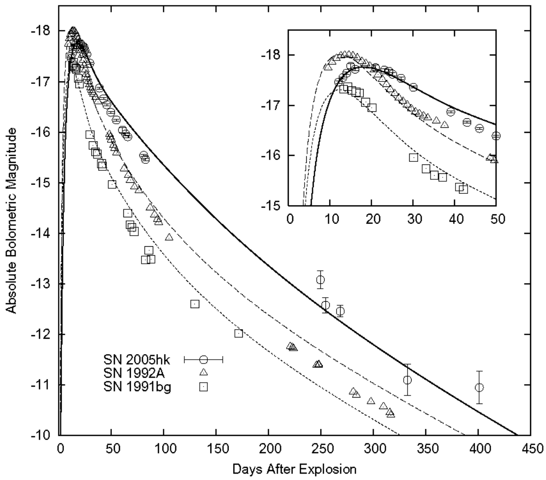

FIGURE 3. The bolometric light curve (LC) of SN 2005hk (circles) compared with a model LC (solid line). Triangles and squares are bolometric LCs of SNe 1992A and 1991bg [27], respectively. Model LCs for these two SNe are shown in dashed and dotted lines, respectively. In order to fix the rise time of the LCs of SNe 1992A and 1991bg, B-band rise time is assumed as $t_{\rm rise} = 19.5 \times s$ days [2], where s is stretch factor of B band LC [4]. The B-band rise times of SNe 1992A ($s = 0.80$) and 1991bg ($s = 0.68$) are estimated as 15.6 and 13.2 days, respectively. Since the LC of SN 2005hk is deviated from the normal sequence of SNe Ia, we simply assume $t_{\rm rise} = 17$ days as in [21].

PECULIAR SUPERNOVA 2005hk

SN 2005hk belongs to a 2002cx-like peculiar group of SNe Ia [12, 10] that shares the following special properties: (1) the slow declining light curve (LC) despite the underluminous peak magnitude, (2) low line velocities, being about a half of normal SNe Ia, and (3) the peculiar late phase spectra ($>$ 300 days after the explosion) that do not resemble those of SNe Ia.

We performed photometric (UBVRI) and spectroscopic observations of SN 2005hk using the 2m Himalayan Chandra Telescope (HCT) and the Subaru telescope. Our data cover the phase from -6 to $+380$ days since B maximum. Detailed behavior of the LCs and early phase spectra will be presented in [23].

Light Curve

The bolometric LC constructed with our data and published NIR data [21] is shown in Figure 3 (circles). Its faintness at maximum ($M_{bol} \sim -17.7$) certainly indicates that the synthesized mass of ^{56}Ni is as small as $\lesssim 0.2 M_{\odot}$. The decline of the bolometric LC after the maximum is slower than that of SN 1992A (triangles) [27]. The time scale of the bolometric LC ($\tau_{\rm LC}$) is scaled as $\tau_{\rm LC} \propto M_{\rm ej}^{3/4} E_{\rm K}^{-1/4}$ [1], where $M_{\rm ej}$ is the mass of the

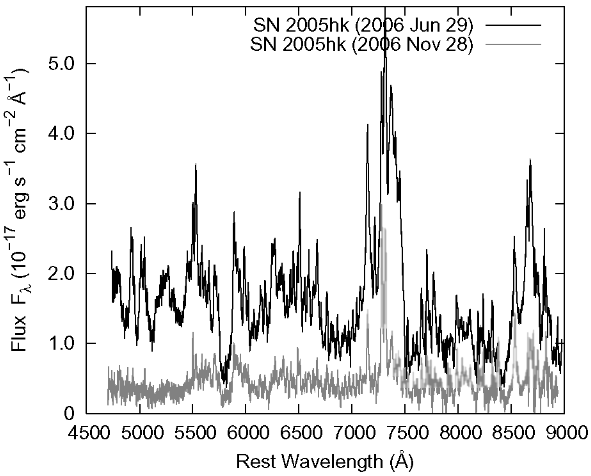

FIGURE 4. Late phase spectra of SN 2005hk taken by Subaru telescope.

ejecta and E_K is the kinetic energy of the ejecta.

If the ejecta mass (M_{ej}) is similar to that of normal SNe Ia (Chandrasekhar mass), the slow decline suggests that SN 2005hk has a much smaller kinetic energy, which is consistent with the low expansion velocity. Phillips et al. [21] confirmed this hypothesis by modeling the LC until 80 days after the explosion.

Figure 3 shows the late phase light curve of SN 2005hk. At $t > 250$ days after the explosion, the bolometric luminosity of SN 2005hk is brighter than that of SN 1992A by ~ 1 magnitude. This implies that γ-rays from decaying ^{56}Co are more efficiently trapped than in SN 1992A. This fact also suggests that SN 2005hk has a much lower explosion energy than normal SNe Ia.

To estimate the kinetic energy quantitatively, we compute synthetic bolometric LCs with an LTE radiation hydrodynamics and a gray γ-ray transfer code [9]. The line opacity is assumed to be constant (0.1 cm^2 g^{-1}) for simplicity. We use W7 deflagration model [17] as a standard density structure and abundance distributions.

First, the mass of ^{56}Ni [$M(^{56}\mathrm{Ni})$] is varied to obtain good agreement with the maximum luminosity. The dashed and dotted lines in Figure 3 are synthetic LCs with $M(^{56}\mathrm{Ni}) = 0.17$ and $0.088 M_\odot$, respectively. Both at early phase (see the inset of Figure 3) and at late phase, these LCs are in good agreement with SNe 1992A and SN 1991bg [27], respectively. However, the model sequence with various $M(^{56}\mathrm{Ni})$ never reproduces the brightness of SN 2005hk at $\gtrsim 50$ days after the explosion.

Secondly, we try to explain the LC of SN 2005hk with less energetic models by homologously scaling the structure of W7. The solid line in Figure 3 is the synthetic LC for $M(^{56}\mathrm{Ni}) = 0.18 M_\odot$ and $E_K = 0.3 \times 10^{51}$ergs $= 0.25 \times E_{W7}$, where E_{W7} is the kinetic energy of W7. This kinetic energy is similar to that of the model used in [21]. This model is in a reasonable agreement with SN 2005hk at late phase as well as at early phase, confirming the validity of the low kinetic energy.

Late Phase Spectra

Late phase spectra of SN 2005hk were taken by Subaru telescope on June 29 and November 28, 2006 (Figure 4). They do not show emission features of forbidden lines as in normal SNe Ia. They, in fact, consist of P-cygni profiles. These properties are similar to those of SN 2002cx [10]. The less energetic SN Ia model used in LC analysis contains about $\sim 0.8 M_\odot$ of unburned C and O. Although such model predicts that C and O lines would appear in the late phase, such lines are not seen in observed spectra.

If the ejecta is composed of almost pure Fe-Ni, $M_{\rm ej} \sim M(^{56}{\rm Ni}) \sim 0.2 M_\odot$. By applying Arnett's scaling law $M_{\rm ej}^{3/4} E_{\rm K}^{-1/4}$ [1], the kinetic energy is only $\sim 1/100$ of the model in Figure 4. Then $E/M_{\rm ej}$ would be too small to explain the observed expansion velocity.

Because of the good agreement between the synthetic and observed LCs and spectra of SN 2005hk, the ejected mass and the explosion energy may not be so different from the adopted model, i.e., $M_{\rm ej} \sim 1.4 M_\odot$ and $M(^{56}{\rm Ni}) = 0.18 M_\odot$ unless the opacity is much larger than that adopted in Figure 4. Thus the missing oxygen remains a serious problem.

REFERENCES

1. Arnett, D. *ApJ*, **253**, 785 (1982)
2. Conley, A., et al. *AJ*, **132**, 1707 (2006)
3. Fujimoto, M.Y. *ApJ*, **257**, 752 (1982)
4. Goldhaber, G., et al. *ApJ*, **558**, 359 (2001)
5. Hachisu, I., & Kato, M. *ApJ*, **558**, 323 (2001)
6. Hachisu, I., Kato, M., Nomoto, K., & Umeda, H., *ApJ*, **519**, 314 (1999)
7. Hachisu, I., Kato, M., & Nomoto,K., *ApJ*, **522**, 487 (1999)
8. Hillebrandt, W., & Niemeyer, J. 2000, *ARAA*, **38**, 191 (Errata at http://arjournals.annualreviews.org/doi/abs/10.1146/annurev.aa.38.010100.200001)
9. Iwamoto, K., et al. *ApJ*, **534**, 660 (2000)
10. Jha, S. et al. *AJ*, **132**, 186 (2006)
11. Li, X.-D., & van den Heuvel, E.P.J, *ApJ*, **322**, L9 (1997)
12. Li, W., et al. *PASP*, **115**, 453 (2003)
13. Livio, M. in *Type Ia Supernovae: Theory and Cosmology*, eds. J. Truran & J. Niemeyer (Cambridge: Cambridge Univ. Press), 33 (2000)
14. Nariai, K., Nomoto, K., & Sugimoto, D. *PASJ*, **32**, 473 (1980)
15. Nomoto, K. *ApJ*, **253**, 798 (1982)
16. Nomoto, K., Nariai, K., & Sugimoto, D. *PASJ*, **31**, 287 (1979)
17. Nomoto, K., Thielemann, F.-K., & Yokoi, K. *ApJ*, **286**, 644 (1984)
18. Nomoto, K., et al., in *Type Ia Supernovae: Theory and Cosmology*, eds. J. Truran & J. Niemeyer (Cambridge: Cambridge Univ. Press), 63, astro-ph/0003134 (2000)
19. Nomoto, K., Saio, H., Kato, M., & Hachisu, I. (NSKH) *ApJ*, **664**, in press, astro-ph/0603351 (2007)
20. Paczyński, B., & Żytkow, A.N. *ApJ*, **222**, 604 (1978)
21. Phillips, M. M., et al. *PASP*, in press (astro-ph/0611295)
22. Prialnik, D. *ApJ*, **310**, 222 (1986)
23. Sahu, D. K., et al., in preparation (2007)
24. Sienkiewicz, R. *A&A*, **85**, 295 (1980)
25. Sion, E.M., Acierno, M.J., & Tomczyk, S. *ApJ*, **230**, 832 (1979)
26. Starrfield, S., Timmes, F.X., Hix, W.R., Sion, E.M., Sparks, W.M., & Dwyer, S.J. (S04) *ApJ*, **612**, L53 (2004)
27. Suntzeff, N.B., in *IAU Colloq. 145, Supernovae and Supernova Remnants*, edited by R. McCray & Z. Wang (Cambridge: Cambridge Univ. Press), 41 (1996)